Taylor & Francis
Taylor & Francis Group

Combustion Theory and Modelling

ISSN: 1364-7830 (Print) 1741-3559 (Online) Journal homepage: http://www.tandfonline.com/loi/tctm20

Bifurcation and extinction limit of stretched premixed flames with chain-branching intermediate kinetics and radiative loss

Huangwei Zhang & Zheng Chen

To cite this article: Huangwei Zhang & Zheng Chen (2018): Bifurcation and extinction limit of stretched premixed flames with chain-branching intermediate kinetics and radiative loss, Combustion Theory and Modelling, DOI: 10.1080/13647830.2018.1430380

To link to this article: https://doi.org/10.1080/13647830.2018.1430380

Published online: 28 Feb 2018.

Combustion Theory and Modelling, 2018
https://doi.org/10.1080/13647830.2018.1430380

Bifurcation and extinction limit of stretched premixed flames with chain-branching intermediate kinetics and radiative loss

Huangwei Zhang[a]* and Zheng Chen[b,c]

[a]*Department of Mechanical Engineering, National University of Singapore, Singapore 117576, Singapore;* [b]*State Key Laboratory for Turbulence and Complex Systems, Department of Mechanics and Aerospace Engineering, College of Engineering, Peking University, Beijing 100871, PR China;* [c]*CAPT, College of Engineering, Peking University, Beijing 100871, PR China*

(*Received 1 August 2017; accepted 30 December 2017*)

Premixed counterflow flames with thermally sensitive intermediate kinetics and radiation heat loss are analysed within the framework of large activation energy. Unlike previous studies considering one-step global reaction, two-step chemistry consisting of a chain branching reaction and a recombination reaction is considered here. The correlation between the flame front location and stretch rate is derived. Based on this correlation, the extinction limit and bifurcation characteristics of the strained premixed flame are studied, and the effects of fuel and radical Lewis numbers as well as radiation heat loss are examined. Different flame regimes and their extinction characteristics can be predicted by the present theory. It is found that fuel Lewis number affects the flame bifurcation qualitatively and quantitatively, whereas radical Lewis number only has a quantitative influence. Stretch rates at the stretch and radiation extinction limits respectively decrease and increase with fuel Lewis number before the flammability limit is reached, while the radical Lewis number shows the opposite tendency. In addition, the relation between the standard flammability limit and the limit derived from the strained near stagnation flame is affected by the fuel Lewis number, but not by the radical Lewis number. Meanwhile, the flammability limit increases with decreased fuel Lewis number, but with increased radical Lewis number. Radical behaviours at flame front corresponding to flame bifurcation and extinction are also analysed in this work. It is shown that radical concentration at the flame front, under extinction stretch rate condition, increases with radical Lewis number but decreases with fuel Lewis number. It decreases with increased radiation loss.

Keywords: premixed counterflow flame; extinction limit; flame bifurcation; Lewis number; radiation loss

1. Introduction

Flame extinction is one of the most important fundamental combustion processes. Understanding the extinction mechanism of laminar premixed flames is critical for designing novel combustion technologies (e.g. low NO_X emission combustors), and also for accurately modelling turbulent premixed flames with local and global extinctions. Extinction of laminar premixed flames results from excessive radiation and flame stretch, both of which can lead to an incomplete chemical reaction [1]. Furthermore, flammability limits under specific configurations, like counterflow flames, are related to the extinction limits due to

*Corresponding author. Email: huangwei.zhang@nus.edu.sg

these two factors. Therefore, study of radiative and strained premixed flames is helpful for understanding extinction behaviours.

The mechanisms for extinction of laminar premixed flames caused by the interactions between radiation and stretch were analysed through several theoretical investigations based on irreversible one-step chemistry and different flame configurations [2–7]. These studies provide general conclusions concerning premixed flame extinction. For instance, Sohrab and Law derived an explicit formula of critical Damköhler number at extinction [2]. Buckmaster identified five types of flame bifurcations and found that the inferior flammability limit increases with Lewis number (*Le*) [5]. However, extinction is expected to be considerably affected by the finite-rate chemistry, and apparently theoretical analysis with irreversible one-step reaction cannot examine the chemical kinetics effects on flame extinction. Inclusion of detailed chemistry and species transport properties was therefore tried by different researchers. For instance, considering premixed counterflow methane/air and propane/air flames (corresponding to different *Le*) with detailed mechanisms, Sung and Law [8] reproduced the dual extinction limits and discussed the relations between standard and extended flammability limits under different *Le*. Similar efforts were also made by Guo et al. [9] through simulating counterflow premixed methane/air flames. Ju and his co-workers [10–14] systematically analysed the interactions between flame stretch, Lewis number and radiation loss in bifurcation and extinction of counterflow premixed flames. In their work, the *G*-shaped and *K*-shaped curves (extinction stretch rate versus mixture equivalence ratio) depicting different extinction limits were first demonstrated, and the relations between fundamental flammability limit and flammability limit from counterflow premixed flames with variable *Le* were clarified. The aforementioned numerical computations based on detailed chemistry (e.g. [8–10,14]) reasonably reproduce the measured extinction limits of different premixed flames [15,16]. Moreover, Dixon-Lewis studied the different methane/air flame configurations (i.e. single flame unburnt-to-burnt and twin-flame unburnt-to-unburnt opposed flows) and analysed their flame structures at two extinction limits with low and high stretch rates [17,18]. Dixon-Lewis also discussed the preferential diffusion effect of the near-limit pre-mixtures on their extinction behaviours [18].

The above work with detailed chemistry and transport properties provides information about extinction limit and bifurcation of laminar premixed flames. However, general effects of intermediate kinetics and transport properties on flame extinction have not been studied. Previous studies indicate that thermally sensitive intermediate has a significant impact on near-limit phenomena, such as ignition [19,20] and extinction [21]. Therefore, theoretical analysis about flame bifurcation and extinction considering intermediate kinetics is necessary. Furthermore, extinction identification mainly relies on quantification of some key intermediates, e.g. hydroxyl (OH) and formaldehyde (CH_2O). This technique has been widely adopted in experimental work on turbulent premixed flame extinction, e.g. by Kariuki et al. [22] and by Chaudhuri et al. [23]. However, it is not clear how these species evolve at the critical extinction state and whether they are sufficiently representative in the reaction system for extinction of different flame regimes. Therefore, understanding general behaviours of intermediates in extinction is also important for identifying the onset of premixed flame extinguishment.

In this study, bifurcation and extinction limit of premixed counterflow flames will be analysed by considering chain-branching intermediate kinetics and radiation. The objectives are: (1) to assess the effects of fuel and radical Lewis numbers as well as radiation on premixed counterflow flame bifurcation and extinction; (2) to examine the above-mentioned factors on extinction limit and flammability; and (3) to study the intermediate behaviours in flame bifurcation and extinction. Compared to previous work (e.g. [10,11,14]), the novelty

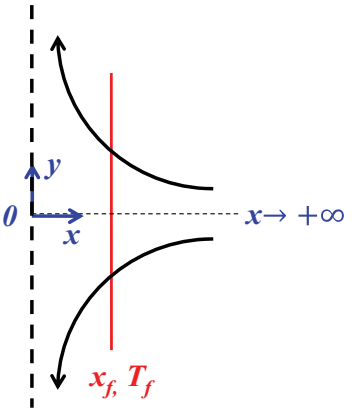

Figure 1. Schematic of the premixed counterflow flame.

of this work is to incorporate generalised thermally sensitive intermediate kinetics, which may enrich our existing appreciation of extinction and flammability limits of stretched premixed flames. The rest of the paper is structured as follows: mathematical models and theoretical analysis are given in Sections 2 and 3, respectively; results and discussion are presented in Section 4; and finally the conclusions are summarised in Section 5.

2. Mathematical models

To consider the radical kinetics in the radiative premixed counterflow flame, a chemical mechanism containing chain-branching reactions should be included. In the present work, the simplified form of the Zel'dovich-Liñán model [24,25] proposed by Dold and co-workers [26–29] is used as the chemical model. It consists of two steps:

$$F + Z \rightarrow 2Z : \; k_B = A_B \, exp\left(-\frac{T_B}{T}\right), \tag{1a}$$

$$Z + M \rightarrow P + M : \; k_C = A_C, \tag{1b}$$

where F, Z, P, and M represent fuel, intermediate (or radical; they will be used interchangeably hereafter), product, and any third body, respectively. A_B and T_B are the frequency factor and activation temperature of Reaction (1a), respectively, while A_C the frequency factor of Reaction (1b). The simplified Zel'dovich-Liñán model consists of a thermally sensitive chain branching Reaction (1a) with a rate constant k_B in Arrhenius form and a completion Reaction (1b) with a rate constant k_C which is equal to the frequency factor A_C and does not depend on temperature T. The applications of this model and its extended version can be found in previous studies on ignition, extinction and propagation of premixed spherical flames, flame balls and freely propagating planar flames [19,20,26–34].

The premixed counterflow flame is considered here. In this configuration, twin flames are formed around the stagnation plane located at $x = 0$ (where x is the streamwise coordinate as shown in Figure 1). Due to the symmetry, only half of the domain, i.e. $x \in [0, +\infty)$, is taken into consideration (see Figure 1). Similar to our previous theoretical analysis [19,20,34,35], constant properties are assumed for density ρ, specific heat C_P, diffusion coefficients of fuel D_F and radical D_Z, thermal conductivity λ, and heat of reaction Q. Based

on the classical reactive-diffusive model and the two-step chemistry in Reactions (1a) and (1b), the one-dimensional equations for mass fractions of fuel, Y_F, and radical, Y_Z, as well as temperature T, are:

$$\rho u \frac{\partial Y_F}{\partial x} = \frac{\partial}{\partial x}\left(\rho D_F \frac{\partial Y_F}{\partial x}\right) - W_F \omega_B, \tag{2a}$$

$$\rho u \frac{\partial Y_Z}{\partial x} = \frac{\partial}{\partial x}\left(\rho D_Z \frac{\partial Y_Z}{\partial x}\right) + W_Z\left(\omega_B - \omega_C\right), \tag{2b}$$

$$\rho C_P u \frac{\partial T}{\partial x} = \frac{\partial}{\partial x}\left(\lambda \frac{\partial T}{\partial x}\right) + Q\omega_C - L. \tag{2c}$$

In Equations (2a)–(2c), $u = -kx$ is the streamwise velocity and k is the stretch rate. The reaction rates ω_B and ω_C are [27,29]:

$$\omega_B = \frac{\rho Y_F}{W_F}\frac{\rho Y_Z}{W_Z} A_B exp\left(-\frac{T_B}{T}\right) \text{ and } \omega_C = \frac{\rho}{W}\frac{\rho Y_Z}{W_Z} A_C, \tag{3}$$

where W_F and W_Z are the molecular weights of fuel and radical, respectively, and W represents the mean molecular weight. In addition, L denotes the radiative heat loss and, for simplicity, is assumed to linearly depend on the temperature, i.e. $L = hT$. h is radiation loss coefficient. This approximation has also been used by Dold and his co-workers with the same chemical model [26–29]. In [35] this linear radiation model was compared to the quartic radiation model ($L \sim T^4$) and both models were found to yield qualitatively and quantitatively similar results. However, according to the asymptotic analysis based on one-step chemistry by Ju et al. [36], the linearised approximation may lead to under-prediction of the flammability limit.

Following Dold et al. [27], we introduce the following non-dimensional variables to normalise Equations (2a)–(2c):

$$x^{'} = \frac{x}{x_s},\ T^{'} = \frac{T - T_0}{T_s},\ Y_F^{'} = \frac{Y_F}{Y_{F0}},\ Y_Z^{'} = \frac{Y_Z}{Y_{Zs}},\ k^{'} = kt_s,\ L^{'} = \frac{WL}{T_s \rho^2 C_P A_C}, \tag{4}$$

along with the following definitions:

$$t_s = \frac{x_s^2}{\lambda/(\rho C_P)},\ x_s = \sqrt{\frac{\lambda W}{\rho^2 C_P A_C}},\ Y_{Zs} = \frac{W_Z Y_{F0}}{W_F},\ Q^{'} = \frac{QY_{F0}}{C_P T_s W_F},$$
$$\beta = \frac{T_B T_s}{(T_0 + T_s)^2}, \sigma = \frac{T_s}{T_0 + T_s}. \tag{5}$$

Here T_0 and Y_{F0} are, respectively, the temperature and fuel mass fraction in the fresh mixture. The Zel'dovich number, β, defined in Equation (5) is based on the reference temperature $T_0 + T_s$, instead of the adiabatic flame temperature [26,29]. Following the work in [26,29], the scaling temperature, Ts, is chosen so that $\omega_B = \beta^2 \omega_C$ at the temperature of $T_0 + T_s$, i.e.:

$$\frac{A_B W}{A_C W_F} Y_{F0} = \beta^2\, exp\left(\frac{T_B}{T_0 + T_s}\right). \tag{6}$$

The non-dimensional equations for mass fractions of fuel and radical, Y_F and Y_Z, as well as temperature, T, read (the prime superscripts are dropped for brevity):

$$-kx\,\frac{dY_F}{dx} = \frac{1}{Le_F}\,\frac{d^2Y_F}{dx^2} - \omega, \tag{7a}$$

$$-kx\,\frac{dY_Z}{dx} = \frac{1}{Le_Z}\,\frac{d^2Y_Z}{dx^2} + \omega - Y_Z, \tag{7b}$$

$$-kx\,\frac{dT}{dx} = \frac{d^2T}{dx^2} + QY_Z - L, \tag{7c}$$

with the non-dimensional reaction rate ω written as [27]:

$$\omega = \beta^2\, Y_F Y_Z exp\left[\beta\frac{T-1}{1+\sigma\,(T-1)}\right]. \tag{8}$$

The boundary conditions at $x = 0$ and $x \to +\infty$ are:

$$x = 0: \quad \frac{dT}{dx} = \frac{dY_F}{dx} = \frac{dY_Z}{dx} = 0, \tag{9a}$$

$$x \to +\infty : T = 0, \quad Y_F = 1, \quad Y_Z = 0. \tag{9b}$$

In the limit of large activation energy ($\beta\to+\infty$), chemical reactions are confined at an infinitesimally thin flame sheet ($x = x_f$) and beyond that the flow is chemically frozen. Based on the asymptotic analysis conducted by Dold and his co-workers [26,29], the following conditions must be valid across or at the flame front ($x = x_f$):

$$[Y_F] = [Y_Z] = [T] = T - 1 = \left[\frac{dT}{dx}\right] = \left[\frac{1}{Le_F}\frac{dY_F}{dx} + \frac{1}{Le_Z}\frac{dY_Z}{dx}\right] = Y_F\,\frac{dT}{dx} = 0, \tag{10}$$

where the square brackets denote the difference between the variables on the unburned and burned sides, i.e. $[f] = f(x = x_f^+) - f(x = x_f^-)$.

3. Asymptotic analysis

With the assumption of large activation energy ($\beta\to+\infty$) and hence frozen chemistry beyond the flame sheet ($\omega = 0$ if $x \neq x_f$), Equations (7a)–(7c) can be written in the following form:

$$-kx\,\frac{dY_F}{dx} = \frac{1}{Le_F}\,\frac{d^2Y_F}{dx^2}, \tag{11a}$$

$$-kx\,\frac{dY_Z}{dx} = \frac{1}{Le_Z}\,\frac{d^2Y_Z}{dx^2} - Y_Z, \tag{11b}$$

$$-kx\,\frac{dT}{dx} = \frac{d^2T}{dx^2} + QY_Z - hT. \tag{11c}$$

Equations (11a)–(11c), together with boundary and jump conditions in Equations (9a), (9b) and (10), can be solved analytically in the burned ($0 \le x < x_f$) and unburned ($x_f < x < +\infty$) zones, respectively.

The exact solutions for the mass fraction of fuel $Y_F(x)$ are:

$$Y_F(x) = \begin{cases} 0, & \text{if } 0 \le x < x_f \\ \dfrac{erf\left(\sqrt{\frac{Le_F k}{2}}x_f\right) - erf\left(\sqrt{\frac{Le_F k}{2}}x\right)}{erf\left(\sqrt{\frac{Le_F k}{2}}x_f\right) - 1}, & \text{if } x_f < x < +\infty \end{cases} \tag{12}$$

where $erf(\tau) = \frac{2}{\sqrt{\pi}} \int_0^{\tau} e^{-t^2} dt$ is the error function.

The distributions of the radical mass fraction $Y_Z(x)$ are given by:

$$Y_Z(x) = \begin{cases} Y_{zf} e^{\frac{1}{2} Le_Z k\left(x_f^2 - x^2\right)} \dfrac{J^+\left(\frac{1}{k'}\sqrt{\frac{Le_Z k}{2}}x\right) + J^-\left(\frac{1}{k'}\sqrt{\frac{Le_Z k}{2}}x\right)}{J^+\left(\frac{1}{k'}\sqrt{\frac{Le_Z k}{2}}x_f\right) + J^-\left(\frac{1}{k'}\sqrt{\frac{Le_Z k}{2}}x_f\right)}, & \text{if } 0 \le x < x_f \\ Y_{zf} e^{\frac{1}{2} Le_Z k\left(x_f^2 - x^2\right)} \dfrac{J^-\left(\frac{1}{k'}\sqrt{\frac{Le_Z k}{2}}x\right)}{J^-\left(\frac{1}{k'}\sqrt{\frac{Le_Z k}{2}}x_f\right)}, & \text{if } x_f < x < +\infty \end{cases} \tag{13}$$

where $J^-(a,b) = \int_0^{\infty} \varsigma^a e^{(-\frac{1}{4}\varsigma^2 - b\varsigma)} d\varsigma$ and $J^+(a,b) = \int_0^{\infty} \varsigma^a e^{(-\frac{1}{4}\varsigma^2 + b\varsigma)} d\varsigma$. Y_{Zf} in Equation (13) is the radical mass fraction at the flame front $x = x_f$, i.e. $Y_Z(x = x_f) = Y_{Zf}$. Substituting Equations (12) and (13) into the condition of $[\frac{1}{Le_F}\frac{dY_F}{dx} + \frac{1}{Le_Z}\frac{dY_Z}{dx}] = 0$ at $x = x_f$ from Equation (10) yields the following expression for Y_{Zf}:

$$Y_{Zf} = \frac{\frac{\sqrt{\frac{2Le_Z}{k}} e^{-\frac{1}{2} Le_F k x_f^2}}{Le_F \int_{x_f}^{+\infty} e^{-\frac{1}{2} Le_F k \tau^2} d\tau}}{\frac{J^+\left(1 + \frac{1}{k'}\sqrt{\frac{Le_Z k}{2}}x_f\right) - J^-\left(1 + \frac{1}{k'}\sqrt{\frac{Le_Z k}{2}}x_f\right)}{J^-\left(\frac{1}{k'}\sqrt{\frac{Le_Z k}{2}}x_f\right) + J^+\left(\frac{1}{k'}\sqrt{\frac{Le_Z k}{2}}x_f\right)} + \frac{J^-\left(1 + \frac{1}{k'}\sqrt{\frac{Le_Z k}{2}}x_f\right)}{J^-\left(\frac{1}{k'}\sqrt{\frac{Le_Z k}{2}}x_f\right)}} \tag{14}$$

The radiation heat loss is comparatively smaller than convection and diffusion terms [5,6,37]. Therefore, the radiation loss coefficient h is a small quantity, i.e. $h \ll 1$, and one can expand temperature $T(x)$ in the burned and unburned zones with respect to small radiation loss coefficient h, i.e. $T(x) = T_0(x) + h \cdot T_1(x) + O(h^2)$. The full expression for $T(x)$ is (terms of $O(h^2)$ are neglected):

$$T(x) = \begin{cases} \underbrace{1 + \int_x^{x_f}\int_0^{\eta} I_1(\xi,\eta)\, d\xi d\eta}_{T_0(x)} + h \cdot \underbrace{(-1)\int_x^{x_f}\int_0^{\eta} I_2(\xi,\eta)\, d\xi d\eta}_{T_1(x)}, & \text{if } 0 \le x < x_f \\ \underbrace{\dfrac{\int_x^{+\infty} e^{-\frac{1}{2}\xi^2 k} d\xi}{\int_{x_f}^{+\infty} e^{-\frac{1}{2}\xi^2 k} d\xi}\left[1 + \int_{x_f}^{+\infty}\int_{\eta}^{+\infty} I_1(\xi,\eta)\, d\xi d\eta\right] - \int_x^{+\infty}\int_{\eta}^{+\infty} I_1(\xi,\eta)\, d\xi d\eta}_{T_0(x)} \\ \quad + h \cdot \underbrace{\dfrac{\int_x^{+\infty} e^{-\frac{1}{2}\varsigma^2 k} \int_{x_f}^{+\infty}\int_{\varsigma}^{\eta} I_2(\xi,\eta)\, d\xi d\eta d\varsigma}{\int_{x_f}^{+\infty} e^{-\frac{1}{2}\xi^2 k} d\xi}}_{T_1(x)}, & \text{if } x_f < x < +\infty \end{cases} \tag{15}$$

in which $I_1(\xi, \eta)$ and $I_2(\xi, \eta)$ are:

$$I_1\ (\xi, \eta) = \ QY_Z\,(\xi)\, e^{\frac{1}{2}k\left(\xi^2-\eta^2\right)} \text{ and } I_2\ (\xi, \eta) = T_0\ (\xi)\, e^{\frac{1}{2}k\left(\xi^2-\eta^2\right)}. \tag{16}$$

The temperature jump condition of $[\frac{dT}{dx}] = 0$ at the flame front $x = x_f$ is used and we obtain the following implicit correlation between flame front location x_f and flame stretch k:

$$\int_{x_f}^{+\infty}\int_{0}^{\eta} [I_1(\xi, \eta) - h \cdot I_2(\xi, \eta)]\, d\xi d\eta = 1. \tag{17}$$

According to Equation (17), for given radiation loss coefficient h, heat of reaction Q, fuel Lewis number Le_F, and radical Lewis number Le_Z, we can get x_f as a function of k, and furthermore the flame speed s_u based on $s_u = k \cdot x_f$.

Equation (17) can be numerically evaluated, and therefore the effects of fuel Le_F, Le_Z, and Q on bifurcation and extinction of premixed counterflow flames considering radiation and thermally sensitive intermediate kinetics can be assessed. In the current investigations, the heat of reaction Q is set to be 2.0. This value is close to that of a typical hydrocarbon mixture with initial temperature of 300–500 K [29].

For the adiabatic premixed counterflow flames ($h = 0$), the correlation between x_f and k in Equation (17) can be simplified to:

$$\int_{x_f}^{+\infty}\int_{0}^{\eta} I_1(\xi, \eta)\, d\xi d\eta = 1. \tag{18}$$

To assist the discussion in Section 4, the results for the freely propagating planar flame are also presented here. They are obtained from similar equations to Equations (11a)–(11c) (in which kx is replaced by the propagating speed, U, of the planar flame), together with the boundary and jump conditions, i.e. Equations (9a), (9b) and (10). The correlation between the planar flame propagating speed U, radical Lewis numbers, Le_Z, and heat of reaction Q is:

$$\lambda_1 + \frac{QY_{zf}^0\,(\lambda_1 - \gamma_1)}{\gamma_1^2 + U\gamma_1 - h} = \lambda_2 + \frac{QY_{zf}^0\,(\lambda_2 - \gamma_2)}{\gamma_2^2 + U\gamma_2 - h}, \tag{19}$$

in which:

$$Y_{zf}^0 = \frac{Le_Z U}{\gamma_1 - \gamma_2},\ \lambda_1 = \frac{-U + \sqrt{U^2 + 4h}}{2},\ \lambda_2 = \frac{-U - \sqrt{U^2 + 4h}}{2},$$
$$\gamma_1 = \frac{-ULe_Z + \sqrt{(ULe_Z)^2 + 4Le_Z}}{2},\ \gamma_2 = \frac{-ULe_Z - \sqrt{(ULe_Z)^2 + 4Le_Z}}{2}. \tag{20}$$

It is noted that the correlation for the unstrained planar flame, Equation (19), is independent of Le_F and Q. Moreover, Y_{zf}^0 is only affected by Le_Z. The above results for planar flames are the same as those in [29].

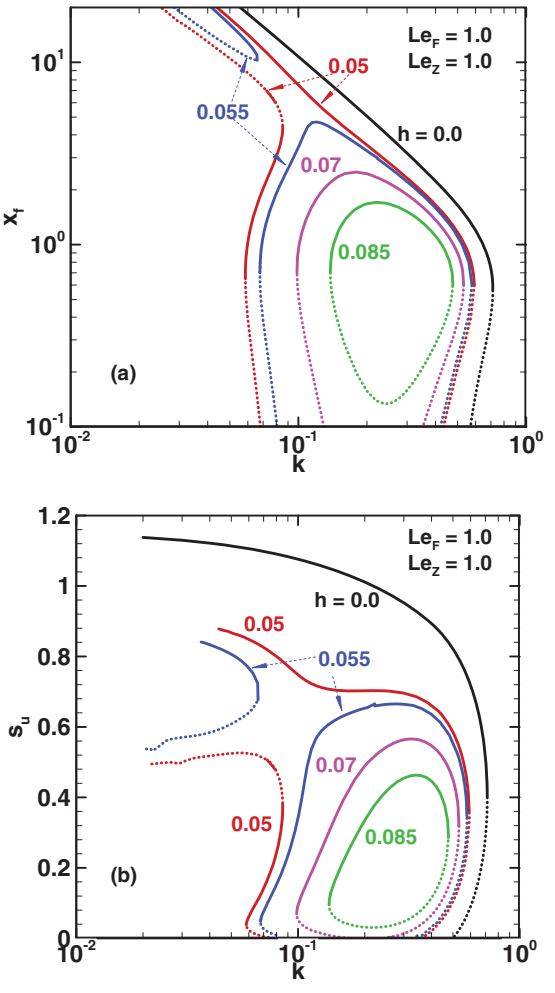

Figure 2. Flame location (a) and flame speed (b) as a function of flame stretch for variable radiation coefficients. $Le_F = Le_Z = 1.0$. Solid curves: stable flame; dashed curves: unstable flame. The legend for curve type also applies for Figures 3–6 and Figure 11 .

4. Results and discussion

4.1. *Flame bifurcation and flammable region*

The location of premixed counterflow flame, x_f, as a function of flame stretch, k, is plotted in Figure 2(a) for $Le_F = Le_Z = 1.0$. For adiabatic flame with $h = 0$, only one reverse C-shaped branch of solutions is obtained. For a small or intermediate stretch rate k, there are two possible flame locations x_f, demarcated by a turning point, as shown in Figure 2(a). Based on the bifurcation theory [38], the upper branch (solid line) is physically stable, whereas the lower branch (dashed line) is unstable. When the stretch rate is beyond the turning point, no flame solutions exist. This is the stretch induced extinction limit, $k_{s,ext}$, which is caused by short residence time. For adiabatic flame, the flammable region is $k < k_{s,ext}$.

For radiative flame with $h = 0.05$, there is a new Z-shaped flame branch on the left, which has two turning points. Based on the general bifurcation knowledge [38], the middle section with approximately $0.06 < k < 0.08$ denotes the physical stable flame solutions, whereas the upper and lower sections are unstable. When k is lower than the stretch rate at the lower turning point of the left branch, no flame solution exists. This turning point corresponds to the so-called radiation induced extinction limit, $k_{r,ext}$. Different from the stretch induced extinction limit at the right branch, this extinction is caused by the increased contribution of radiation due to the decreased stretch and therefore increased flame thickness [14]. Along the Z-shaped branch, if k is increased beyond the upper turning point, the flame solution would jump vertically to the right branch. In Figure 2(a), the flame bifurcation curves of $h = 0.05$ are similar to the open-mushroomed curves for non-adiabatic stretched CH_4/air premixed flames with $Le \approx 1.0$ obtained from simulations by Ju et al. [10].

At $h = 0.055$, new flame bifurcation occurs: the upper and lower branches emerge, through merging the left and right branches for smaller h (e.g. $h = 0.05$). Here we define the radiation loss coefficient h with which merging of two branches critically occurs as the merging limit. In this case, both branches have physically stable flame solutions. The stable flame solutions along the upper branch were called the far standing weakly stretched flame (FSWSF) by Ju et al. [10]. At the turning point the FSWSF jumps to the lower branch (called the near stagnation flame (NSF) by Ju et al. [10]). This jump is caused by the increased radiation loss. NSF solutions are confined by the left extinction limit due to radiation and right limit due to the high stretch.

For $h = 0.07$ and 0.085, only NSF branches appear and thereby the flammable regions shrink greatly. When the radiation loss coefficient h is greater than 0.085, two limits merge and the flammability limit of this counterflow flame is reached. It is noted that the upper branches, FSWSF, only exist for a relatively narrow range of h before it is degraded with the flammability limit from unstretched planar flame (hereafter termed standard flammability limit), and for $h = 0.07$ and 0.085, there are no FSWSF solutions. This will be further discussed for Figure 10(a). Therefore, this stretched counterflow flame can burn below the standard flammability limit. Extension of flammability limit was also observed in simulations with detailed chemistry for radiative premixed counterflow CH_4/air flames [10], and in micro-gravity experiments for stretched premixed CH_4/air flames [15,16].

The flame speed s_u as a function of k corresponding to $Le_F = Le_Z = 1.0$ is demonstrated in Figure 2(b). For $h = 0$, s_u of the stable flame monotonically decreases when the stretch rate increases and the flame extinguishes with finite flame speed at $k_{s,ext}$. When $h = 0.05$, the flame speed s_u of the right branch first slightly decreases, then increases and finally decreases. It is much higher than that of the left stable weak flame branch. Therefore, the left and right branches are respectively termed weak flame (WF) and normal flame (NF). For $h = 0.055$, the flame speed s_u of FSWSF is higher than that of the NSF. For NSF, at the peak flame location, increasing the flame stretch leads to first slight increase of s_u, which reaches the maximum value at some k, and then decrease until extinction happens. The first increase is caused by the decreased radiation loss intensity, while the ensuing decrease results from the insufficient residence time.

Based on the results in Figure 2, flame bifurcation, extinction limit, flammability limit and flammable region can be obtained through the model presented in Sections 2 and 3. The results from Figure 2 are qualitatively consistent with the findings from theoretical analysis with one-step chemistry, simulations considering detailed chemistry and also measurements (e.g. [5,10,15,16]).

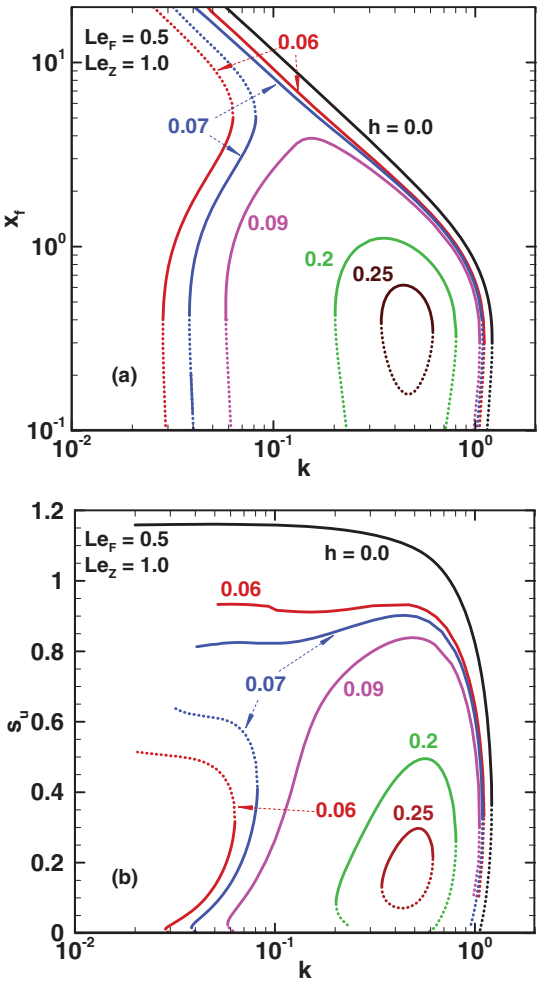

Figure 3. Flame location (a) and flame speed (b) as a function of flame stretch for variable radiation coefficients. $Le_F = 0.5$ and $Le_Z = 1.0$.

4.2. *Effects of fuel and radical Lewis numbers*

Figure 3 shows the flame position x_f and flame speed s_u as functions of flame stretch k with $Le_F = 0.5$ and $Le_Z = 1.0$. Bifurcation curves of adiabatic flame and radiative flames with increased radiation loss coefficients are qualitatively similar to the results with $Le_F = Le_Z = 1.0$ in Figure 2. The differences from the radiative flames needing to be highlighted are as follows. First, between $h = 0.07$ and $h = 0.09$, there is no upper FSWSF stable branch, unlike the one for $h = 0.055$ in Figure 2(a). Second, the radiation loss coefficient h corresponding to the flammability limit, i.e. $h = 0.25$, is much higher than that with $Le_F = Le_Z = 1.0$, i.e. $h = 0.085$. This is because, for $Le_F < 1.0$, intermediate stretch enhances the combustion through the Lewis number effect [1] and the mixture can burn under stronger radiation intensity.

The fuel Lewis number effect is further examined through investigating the flame bifurcations for $Le_F = 2.0$ and $Le_Z = 1.0$ in Figure 4. For the adiabatic flame and radiative

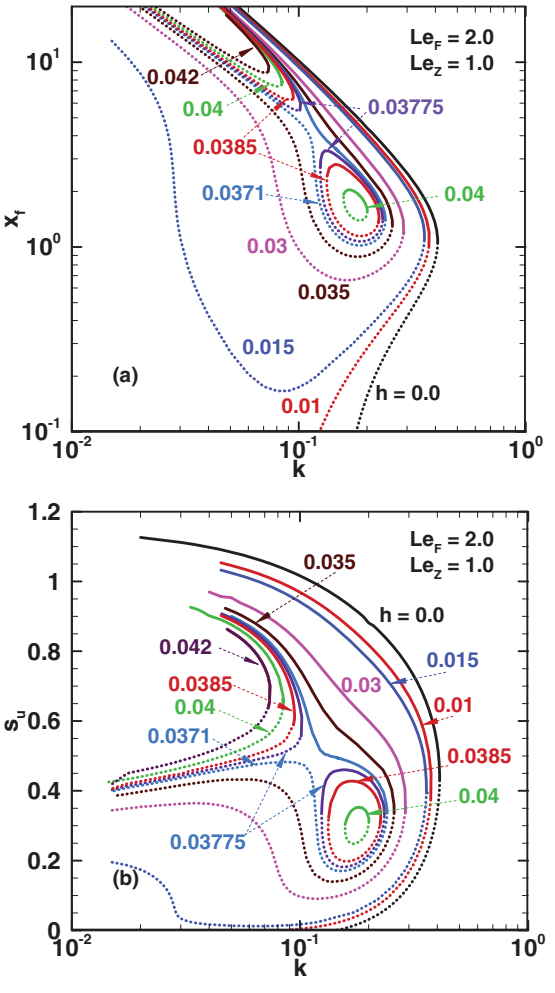

Figure 4. Flame location (a) and flame speed (b) as a function of flame stretch for variable radiation coefficients. $Le_F = 2.0$ and $Le_Z = 1.0$.

one with small h (e.g. $= 0.01$), the x_f–k curve is reverse C-shaped with the turning point being the stretch extinction limit. A new unstable left branch arises at $h = 0.015$. This considerably reduces the flammable region, which becomes smaller when h increases from 0.015 to 0.0371. Figure 4(b) shows that as stretch increases the flame speed s_u decreases monotonically prior to extinction. When h is slightly above 0.0371, the left and right branches merge, generating FSWSF and NSF solutions. When $h = 0.042$, the NSF solutions no longer exist; only with the FSWSF branch. When $Le_F > 1.0$, increasing k weakens the flame through preferential diffusion effect and may also enhance it through reducing the radiation loss. These two effects compete with each other, and in this case the first one dominates the second, thereby making NSF not exist. If h is further increased, then the FSWSF moves left until the standard flammability limit is reached. Therefore, for $Le_F = 2.0$ and $Le_Z = 1.0$, the flammability limit of this counterflow flame equals the standard limit. This finding is consistent with the results reported by Ju et al. [14] who conducted

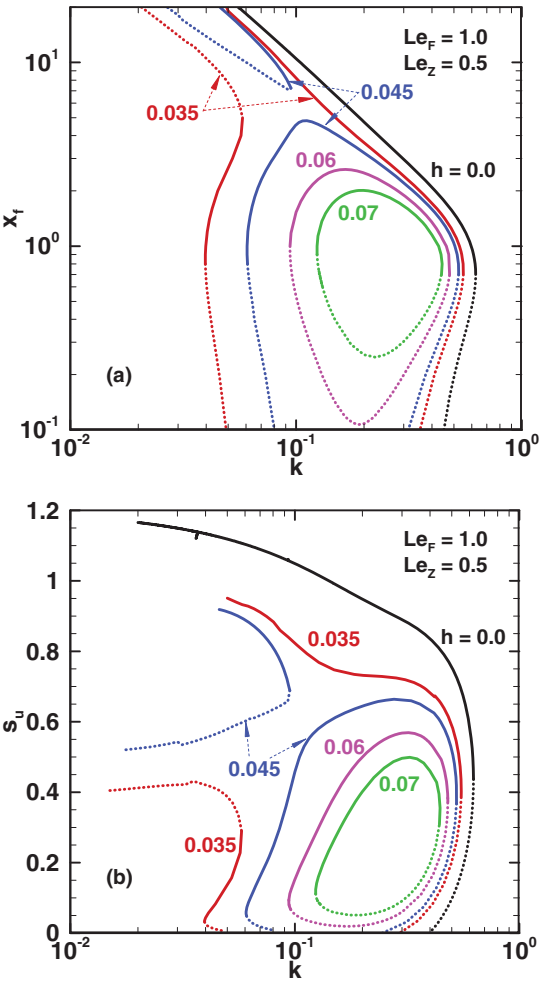

Figure 5. Flame location (a) and flame speed (b) as a function of flame stretch for variable radiation coefficients. $Le_F = 1.0$ and $Le_Z = 0.5$.

simulations for $CH_4/N_2/O_2$/He mixture with $Le = 1.2$ considering detailed chemical and radiation models.

The radical Lewis number effects on bifurcation and extinction of radiative counterflow premixed flames are investigated through changing Le_Z to $Le_Z = 0.5$ in Figure 5 and 2.0 in Figure 6 with fixed $Le_F = 1.0$. When $Le_Z = 0.5$, the x_f–k curves corresponding to adiabatic and radiative flames bifurcate similar to the case with $Le_F = Le_Z = 1.0$ in Figure 2. However, NSF with $Le_F = Le_Z = 1.0$ can exist under larger radiation intensity than this case. Besides, for $h = 0.045$, the turning point on FSWSF branch does not indicate an extinction limit. Instead, if the stretch rate is reduced, the FSWSF would jump to the lower NSF branch.

Figure 6 presents the results for $Le_F = 1.0$ and $Le_Z = 2.0$. The flame bifurcations are qualitatively similar to those in Figure 5, although the flammability limit for the current case is higher. Comparison among results in Figure 2 ($Le_Z = 1.0$), Figure 5 ($Le_Z = 0.5$) and Figure 6 ($Le_Z = 2.0$) indicates that the variations of the radical Lewis number Le_Z do not change the fashion in which the flames bifurcate. Nevertheless, the higher Le_Z, the

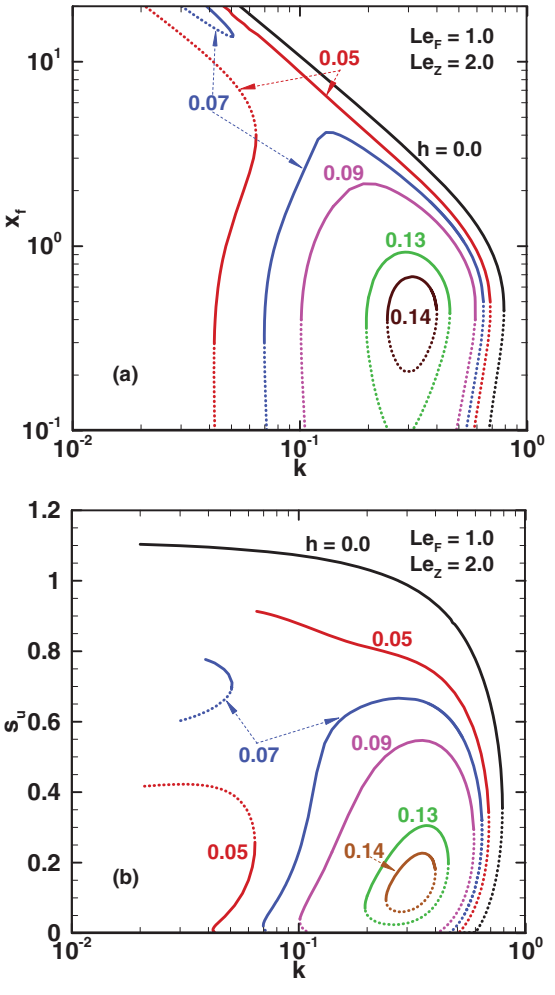

Figure 6. Flame location (a) and flame speed (b) as a function of flame stretch for variable radiation coefficients. $Le_F = 1.0$ and $Le_Z = 2.0$.

larger the flammability limits for the counterflow premixed flame. Higher Le_Z indicates the weaker capacity of radical transport from the flame front and stronger flame reactivity.

4.3. *Extinction and flammability limits*

To generalise the variations of extinction limits demonstrated in Figures 2–6, Figures 7 and 8 show the variations of extinction and radiation stretch rates, $k_{s,ext}$ and $k_{r,ext}$, with Lewis numbers and radiation loss coefficients. In Figure 7, Le_Z is fixed to be unity. For the adiabatic case, $k_{s,ext}$ decreases monotonically with Le_F. When radiation is included with $h = 0.05$ and 0.08, $k_{s,ext}$ also decreases with Le_F, while $k_{r,ext}$ increases with Le_F. The mixture becomes not flammable when fuel Lewis number reaches a critical value, at which $k_{s,ext} = k_{r,ext}$. For $h = 0.05$ and 0.08, these two values correspond to the flammability limits for $Le_F = 1.7$ and 1.2, respectively. It is noted that in Figure 7 $k_{s,ext}$ is from the NF, whereas $k_{r,ext}$ may be from WF when Le_F is relatively small, or be from NSF when the flame approaches the

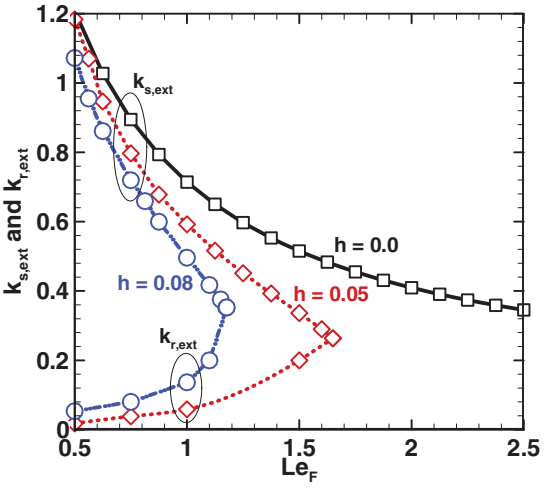

Figure 7. Extinction stretch rate as a function of fuel Lewis number for adiabatic ($h = 0$) and radiative ($h = 0.05$ and 0.08) flames. $Le_Z = 1.0$.

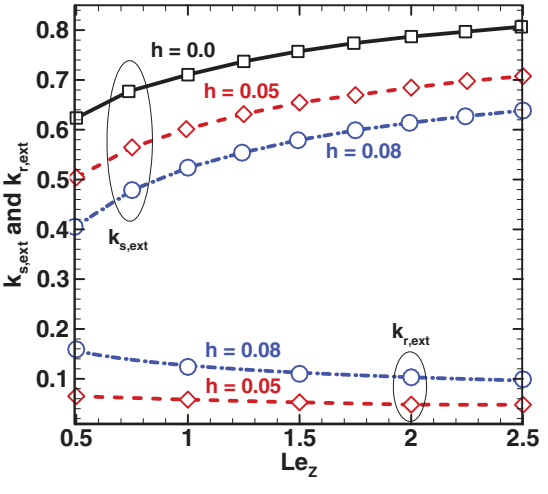

Figure 8. Extinction stretch rate as a function of fuel Lewis number for adiabatic ($h = 0$) and radiative ($h = 0.05$ and 0.08) flames. $Le_F = 1.0$.

flammability limit. Figure 8 shows the variations of $k_{s,ext}$ and $k_{r,ext}$ for different Le_Z and h with $Le_F = 1.0$. Here $k_{s,ext}$ monotonically decreases when radiation intensity increases, i.e. from $h = 0$ to 0.08. This tendency is the same as that in Figure 7. Nevertheless, here $k_{s,ext}$ increases with h, and it slightly decreases with Le_Z. Based on the results shown in Figures 7 and 8, the radiation has the considerable influence on both extinction limits $k_{s,ext}$ and $k_{r,ext}$.

The extinction and flammability limit of freely propagating unstrained planar flames are studied for comparison. Figure 9(a) shows the planar flame propagating speeds U as a function of radiation loss coefficients h for different groups of Lewis numbers. When the radiation loss is less than some critical value for all the shown cases, there are two solutions of U: upper stable branch and lower unstable branch. At the turning point, only one solution exists and the flammability limit of planar flame is reached. The planar flame is not affected

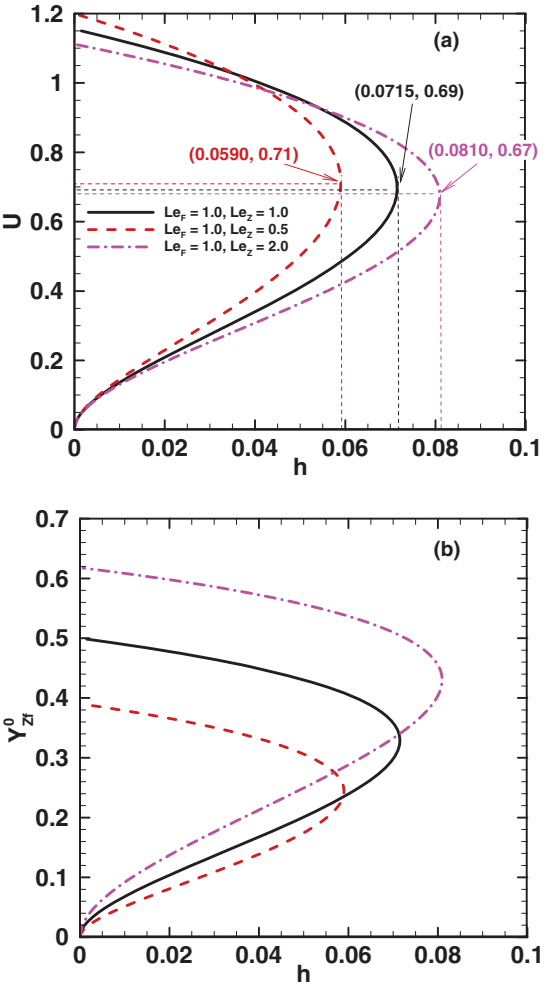

Figure 9. Flame propagation speed (a) and radical mass fraction at the flame front (b) as functions of radiation loss coefficient for variable Lewis numbers of fuel and radical for planar unstretched flames. The number pairs in the parentheses in (a) are the flame speeds and radiation loss coefficients at the turning points.

by Le_F. However, its flammability limit increases with Le_Z. This implies the effects of the radical transport on the extinction and flammability limit of stretched laminar premixed flames.

Radical mass fraction at unstrained planar flame front, Y^0_{Zf}, is plotted in Figure 9(b). For the upper stable flames, the increased radiation weakens the flame, quantified by the reduced Y^0_{Zf}, for all the three shown cases. In addition, Le_Z affects Y^0_{Zf} considerably: the higher Le_Z, the higher Y^0_{Zf}. The extinction characteristics of planar flames indicated in Figure 9 will be used below as references for investigations on the counterflow flame.

Figure 10 demonstrates the critical stretch rates k_{ext} (corresponding to the extinction caused by stretch and radiation, as well as the jump limit from WF to NF, or from FSWSF to NSF) as a function of h for the different cases discussed in Figures 2–6. In Figure 10(a) corresponding to $Le_F = Le_Z = 1.0$, when h is lower than the merging limit, the stretch

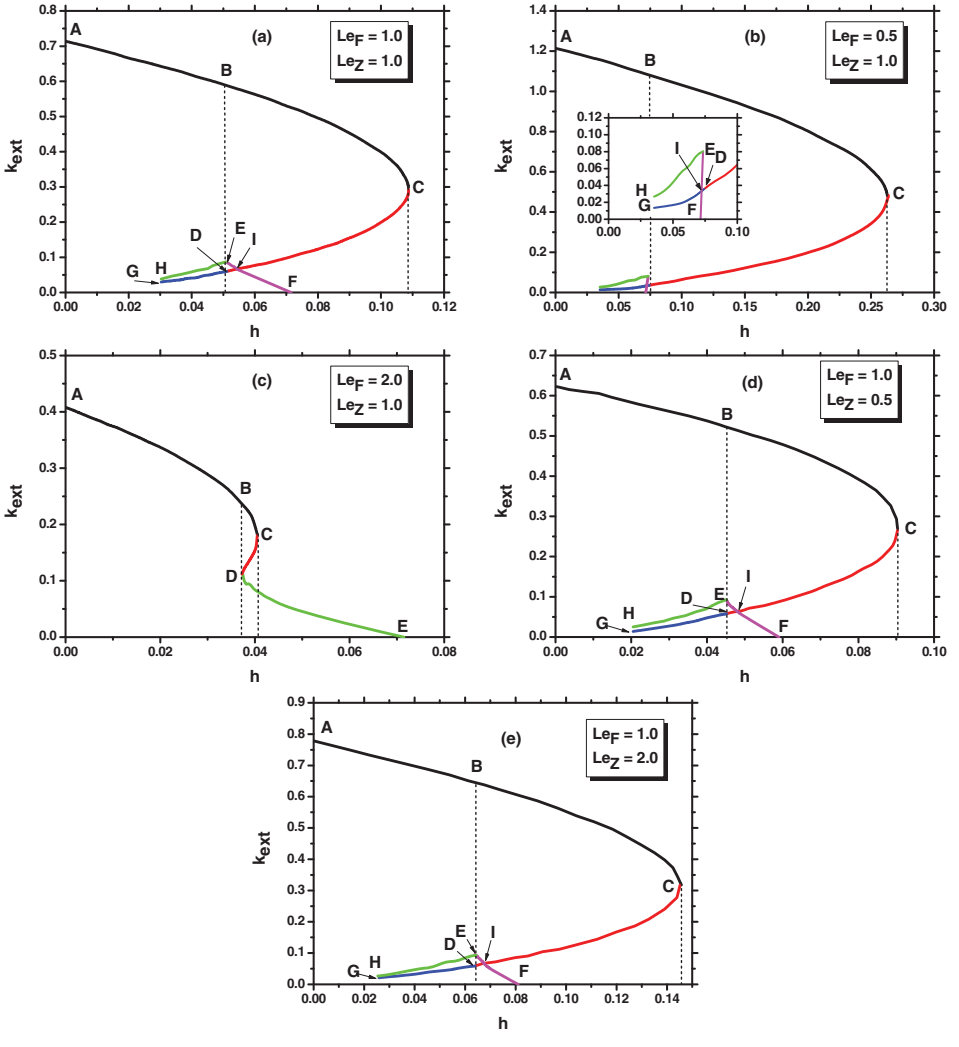

Figure 10. Extinction stretch rate as a function of radiation loss coefficient for variable fuel and radical Lewis numbers. In (a, b, d, e): curves AB: stretch induced extinction limit for NF; BC: radiation extinction limit for NSF; CD: radiation extinction limit for NSF; DG: radiation extinction limit for WF; HE: jump limit for WF; EI: jump limit for FSWSF; IF: extinction limit for FSWSF. In (c): curve AB: stretched extinction limit for NF; stretch extinction limit for NSF; CD: radiation limit for NSF; DE: extinction limit for FSWSF. The left dashed lines: merging limits to produce NSF and FSWSF; the right dashed lines: NSF flammability limit; Point F (Point E in (c)): standard flammability limit from planar premixed flame with zero stretch.

extinction limit of NF, i.e. AB branch in Figure 10(a) (see the curve implications in the caption of Figure 10), decreases with radiation loss coefficient h. The radiation extinction limit and jump limit of WF are characterised by curves DG and HE. When h is smaller, calculations of the WF become difficult and therefore we are not sure how DG and HE are extended at $h \to 0$. Meanwhile, another open question is whether WF would arise even if h is only slightly larger than zero. When h is beyond the merging limit, CD merges with BC at $h \approx 0.11$, the flammability limit for this stretched premixed flame. It is larger than the

standard flammability limit, i.e. $h = 0.071$ (shown in Figure 9(a)) at Point F, extrapolated from the FSWSF extinction limit. The pattern of the extinction curves in Figure 10(a) is similar to those (extinction stretch rate versus mixture equivalence ratio) predicted from stretched CH_4/air flames ($Le \approx 1.0$) based on detailed chemistry [10].

The effects of the fuel Lewis number are demonstrated by Figure 10(b), 10(c), respectively for $Le_F = 0.5$ and $Le_F = 2.0$. For $Le_F = 0.5$, the extinction curve in Figure 10(b) is qualitatively similar to that in Figure 10(a). Quantitatively, h corresponding to the flammability limit at Point C is greater than that with $Le_F = 1.0$. Moreover, the FSWSF only appears for extremely narrow h, close to the merging limit. This justifies why there is no FSWSF in Figure 3(a).

Nevertheless, the extinction curves for $Le_F = 2.0$ in Figure 10(c) are quite different from the previous two. Curve AB is the stretch extinction limit of NF. Additionally, WF is not present here. This is probably caused by the two-step chemistry used here, i.e. Equations (1a) and (1b). Prediction of WF may need detailed chemistry, which can be confirmed from the work with detailed chemistry by Ju et al. [14]. Here NSF (confined by BC and CD) can only exist for a small range of h under large stretch rate when $Le_F > 1.0$. In this case, the extinction limit of FSWSF is the standard flammability limit at Point E, $h = 0.071$. Compared with Figure 10(a), 10(b), the range of h within which FSWSF exists increases with Le_F.

Figure 10(d), 10(e) are plotted for analysing the influence of radical Lewis number on the extinction curves. These curves are qualitatively similar to that of $Le_Z = 1.0$ in Figure 10(a). The flammability limits from the premixed counterflow flame, i.e. the NSF flammability limit at Point C, are extended relative to the standard limits, and increase as Le_Z increases.

4.4. *Radical behaviours in flame bifurcation*

Variations of radical mass fractions at the flame front, Y_{Zf}, with stretch rate k are plotted in Figure 11, corresponding to the five cases in Figures 2–6. Here Y_{Zf} is calculated from Equation (14) based on the solutions in Figures 2–6. For reference, the radical mass fractions at the unstrained planar flame front, Y_{Zf}^0, from Figure 9(b) is also schematically shown. In Figure 11(a) with $Le_F = Le_Z = 1.0$, for the adiabatic case, Y_{Zf} does not change with the stretch rate because of the unity Le_Z. When $h = 0.05$, for the upper NF branch, Y_{Zf} first decreases and then increases with the stretch rate. It is consistently higher than that of the lower WF. At the jump limit (marked with the arrow in Figure 11(a)), Y_{Zf} increases considerably from WF to NF, indicating the sudden change of flame reactivity. For $h = 0.055$, Y_{Zf} of the FSWSF branch shows the monotonic decrease with k, while the NSF branch demonstrates the opposite tendency.

Figure 11(b) and 11(c) demonstrate the Le_F effects on Y_{Zf}. In Figure 11(b), for the adiabatic flame and radiative flames far from flammability limit, Y_{Zf} demonstrates more pronounced increase with increased stretch rate, than that in Figure 11(a). This is related to the combustion enhancement of moderate stretch combined with $Le_F < 1.0$. For $Le_F = 2.0$ in Figure 11(c), Y_{Zf}-k curves are quite different from those in Figure 11(a) and 11(b). For the adiabatic flame and the flames with small h, the stretch reduces Y_{Zf} monotonically, due to $Le_F < 1.0$. Moreover, Y_{Zf} of the NSF solutions decrease when the stretch increases or decreases towards the stretch extinction limit and radiation extinction limit. This differs from the NSF behaviours in Figure 11(a) and 11(b).

The effects of radical Lewis number on the Y_{Zf}-k curves are shown in Figure 11(d) and11(e). They respectively correspond to $Le_Z = 0.5$ and $Le_Z = 2.0$ with $Le_F = 1.0$. The

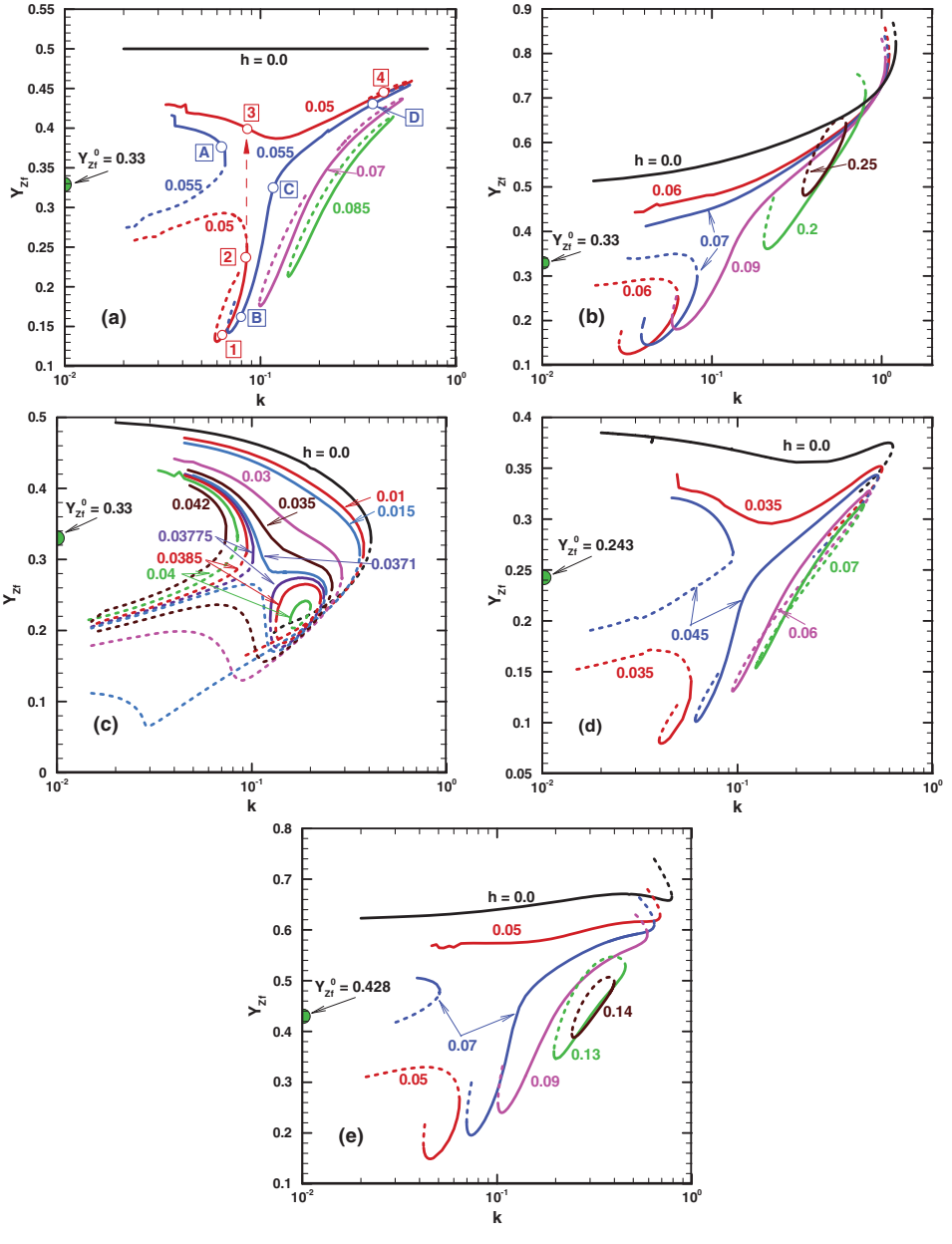

Figure 11. The radical mass fraction at flame front as a function of stretch rate with different Lewis numbers and radiation loss coefficients. (a) $Le_F = 1.0$, $Le_Z = 1.0$; (b) $Le_F = 0.5$, $Le_Z = 1.0$; (c) $Le_F = 2.0$, $Le_Z = 1.0$; (d) $Le_F = 1.0$, $Le_Z = 0.5$; (e) $Le_F = 1.0$, $Le_Z = 2.0$. Y_{Zf}^0 is the radical mass fraction of unstretched planar flame front under the respective Lewis number conditions.

Y_{Zf}-k curves are qualitatively similar to those in Figure 11(a). Nevertheless, the radical mass fractions at both stretch and radiation extinction limits are generally higher with $Le_Z = 0.5$ than those with $Le_Z = 2.0$. This implies the effect of radical transport property on its concentrations when extinction occurs.

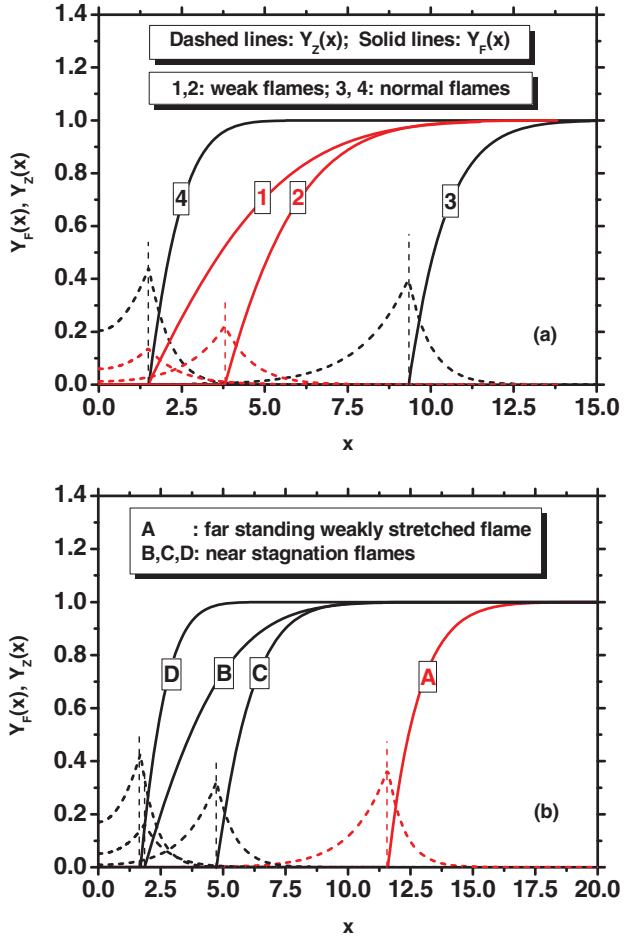

Figure 12. Profiles of fuel and radical mass fractions for (a) weak flames and normal flames, and (b) near stagnation flames and far standing weakly stretched flame. Different flames marked by numbers in (a) and letters in (b) are also indicated in Figure 11(a).

The profiles of fuel and radical mass fractions at the representative flame states for $Le_F = Le_Z = 1.0$ are plotted in Figure 12(a) and 12(b). The numbers 1−4 corresponding to $h = 0.05$ in Figure 12(a) and letters A−D corresponding to $h = 0.055$ in Figure 12(b) are also marked in Figure 11(a). Figure 12(a) compares the flame structures of WF (marked with 1 and 2) and NF (3 and 4). Weak flame 1 is close to the radiation extinction limit, while flame 2 would jump to NF with a slightly higher stretch. The peak radical concentration for flame 1 is higher than that for flame 2. The sudden shift from weak flame 2 to normal flame 3 leads to movement of the flame front off the stagnation plane and the pronounced increase of Y_{Zf}. In addition, normal flame 4 is located at the stretch extinction limit, and its flame location is nearly the same as that of weak flame 1. However, their flame structures differ as shown in Figure 12(a) and normal flame 4 demonstrates stronger reactivity with high Y_{Zf}. The flame structures of FSWSF and NSF are compared in Figure 12(b). A is on the FSWSF branch, and B−D flames on the NSF branch. Moreover, A is near the extinction limit of FSWSF, whereas B and D are close to the radiation and stretch limits of NSF. In

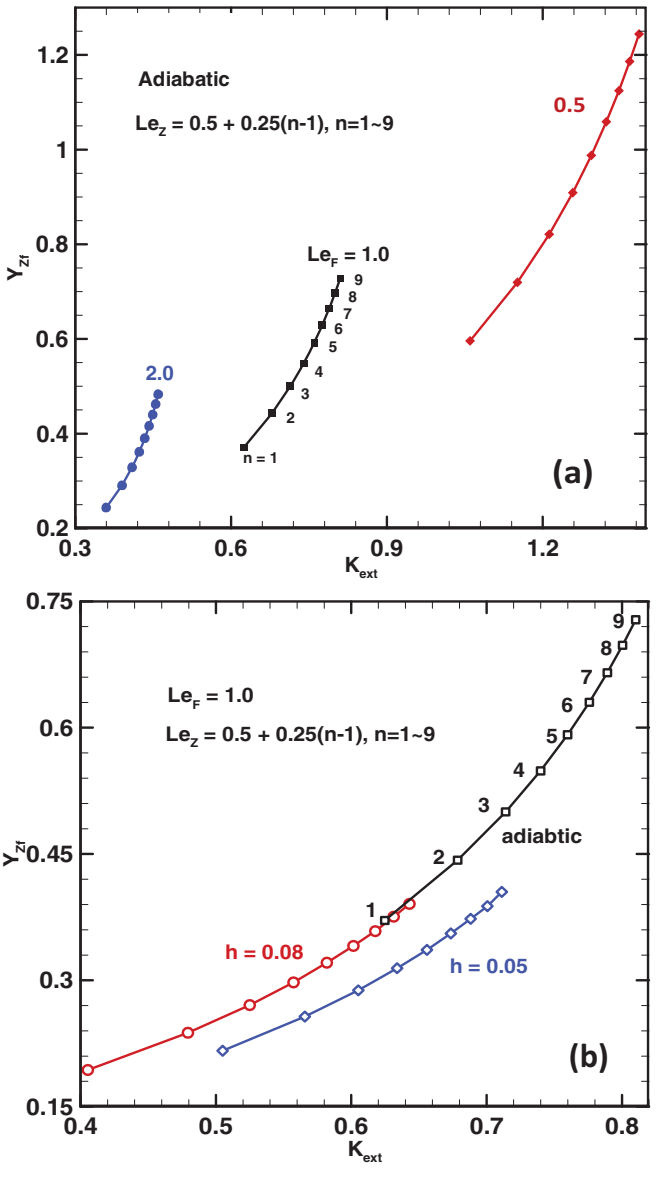

Figure 13. Radical mass fraction as a function of extinction stretch rate for (a) adiabatic and (b) radiative flames with various fuel and radical Lewis numbers.

general, the peak radical mass fraction of A is higher than those of B and C, lower than D. This is consistent with Figure 11(a).

Figure 13 shows radical mass fraction Y_{Zf} at the stretch extinction limits as a function of Lewis numbers and radiation intensities. Figure 13(a) shows the results of the adiabatic flames. Y_{Zf} at different extinction stretch rates monotonically increases with radical Lewis number. Meanwhile, for the same Le_Z, Y_{Zf} becomes larger when the fuel Lewis number is smaller. In Figure 13(b), the influences of radiation on Y_{Zf} are shown. For the same radiation

intensity h, Y_{Zf} at the extinction limit increases with Le_Z. Meanwhile, for the same Le_Z, Y_{Zf} decreases with increased radiation intensity.

5. Conclusions

Bifurcation and extinction limit of premixed counterflow flame considering thermally sensitive intermediate kinetics and radiation heat loss are theoretically studied. The correlation between the flame front location and stretch rate is derived. Based on this correlation, the bifurcation behaviours, extinction limit and flammability limit of the stretched premixed counterflow flame are studied, considering variations of fuel and radical Lewis numbers, as well as radiation heat loss.

The present analysis predicts different flame types and their extinction characteristics, including normal flame, weak flame, near stagnation flame, and far standing weakly stretched flame. It is found that stretch rates at the stretch-induced (radiation-induced) extinction limits deceases (increases) with fuel Lewis number before the flammability limit is reached. The opposite trend is observed for changing radical Lewis number. In addition, the fuel Lewis number shows a significant effect on the relation between the standard flammability limit and the limit corresponding to the strained near stagnation flame. When fuel Lewis number is greater than unity, the flammability limit equals the standard flammability limit; otherwise, it is determined from near stagnation flames. The radical Lewis number has little influence on this relation, though it demonstrates considerable impact on the stretch- and radiation-induced extinction limits. Meanwhile, the flammability limit increases with decreased fuel Lewis number, but with increased radical Lewis number. Radical behaviours at flame front and the corresponding flame structures when flame bifurcation and extinction occur are also studied. It is shown that the Lewis number and radiation heat loss have pronounced effects on radical mass fraction at the flame front. Specifically, under extinction stretch rate condition, radical mass fraction at the flame front increases with radical Lewis number and decreases with fuel Lewis number. Additionally, it decreases with increased radiation loss.

Acknowledgments

HZ gratefully acknowledges the financial support from the start-up grant for the assistant professorship provided by National University of Singapore. ZC is supported by National Natural Science Foundation of China. The authors thank Professor Yiguang Ju from Princeton University for the helpful discussion.

Disclosure statement

No potential conflict of interest was reported by the authors.

Funding

This work was supported by the National Natural Science Foundation of China [grant numbers 91541204, 91741126].

References

[1] C.K. Law, *Combustion Physics*. Cambridge University Press, New York, 2006.
[2] S.H. Sohrab and C.K. Law, *Extinction of premixed flames by stretch and radiative loss*. Int. J. Heat Mass Transf. 27 (1984), pp. 291–300.

[3] B.H. Chao and C.K. Law, *Asymptotic theory of flame extinction with surface radiation*. Combust. Flame 92 (1993), pp. 1–24.
[4] M. Sibulkin and A. Frendi, *Prediction of flammability limit of an unconfined premixed gas in the absence of gravity*. Combust. Flame 82 (1990), pp. 334 –45.
[5] J. Buckmaster, *The effects of radiation on stretched flames*. Combust. Theory Model. 1 (1997), pp. 1–11.
[6] Z. Chen and Y. Ju, *Combined effects of curvature, radiation, and stretch on the extinction of premixed tubular flames*. Int. J. Heat Mass Transf. 51 (2008), pp. 6118–6625.
[7] M. Kitano, H. Kobayashi, and Y. Otsuka, *A study of cylindrical premixed flames with heat loss*. Combust. Flame 76 (1989), pp. 89–105.
[8] C.J. Sung and C.K. Law, *Extinction mechanisms of near-limit premixed flames and extended limits of flammability*. Proc. Combust. Inst. 26 (1996), pp. 865–873.
[9] H. Guo, Y. Ju, K. Maruta, T. Niioka, and F. Liu, *Radiation extinction limit of counterflow premixed lean methane-air flames*. Combust. Flame 109 (1997), pp. 639–646.
[10] Y. Ju, H. Guo, K. Maruta, and F. Liu, *On the extinction limit and flammability limit of non-adiabatic stretched methane-air premixed flames*. J. Fluid Mech. 342 (1997), pp. 315–334.
[11] Y. Ju, H. Guo, K. Maruta, and T. Niioka, *Flame bifurcations and flammable regions of radiative counterflow premixed flames with general Lewis numbers*. Combust. Flame 113 (1998), pp. 603 –14.
[12] Y. Ju, G. Masuya, F. Liu, H. Guo, K. Maruta, and T. Niioka, *Further examinations on extinction and bifurcations of radiative CH4/air and C3H8/air premixed flames*. Proc. Combust. Inst. 27 (1998), pp. 2551–2557.
[13] Y. Ju, C.K. Law, K. Maruta, and T. Niioka, *Radiation-induced instability of strecthed premixed flames*. Proc. Combust. Inst. 28 (2000), pp. 1891–1900.
[14] Y. Ju, H. Guo, F. Liu, and K. Maruta, *Effects of the Lewis number and radiative heat loss on the bifurcation and extinction of CH4/O2-N2-He flames*. J. Fluid Mech. 379 (1999), pp. 165–190.
[15] K. Maruta, M. Yoshida, Y. Ju, and T. Niioka, *Experimental study on methane-air premixed flame extinction at small stretch rates in microgravity*. Proc. Combust. Inst. 16 (1996), pp. 1283–1289.
[16] C.K. Law, D.L. Zhu, and G. Yu, *Propagation and extinction of stretched premixed flames*. Proc. Combust. Inst. 21 (1988), pp. 1419–1426.
[17] G. Dixon-Lewis, *Laminar premixed flame extinction limits. I Combined effects of stretch and upstream heat loss in the twin-flame unburnt-to-unburnt opposed flow configuration*. Proc. R. Soc. London Ser. A Math. Phys. Eng. Sci. 452 (1996), pp. 1857–1884.
[18] G. Dixon-Lewis, *Laminar premixed flame extinction limits. II Combined effects of stretch and radiative loss in the single flame unburnt-to-burnt and the twin-flame unburnt-to-unburnt opposed flow configurations*. Proc. R. Soc. A Math. Phys. Eng. Sci. 462 (2006), pp. 349–370.
[19] H. Zhang and Z. Chen, *Spherical flame initiation and propagation with thermally sensitive intermediate kinetics*. Combust. Flame 158 (2011), pp. 1520–1531.
[20] H. Zhang, P. Guo, and Z. Chen, *Critical condition for the ignition of reactant mixture by radical deposition*. Proc. Combust. Inst. 34 (2013), pp. 3267–3275.
[21] B. Bai, Z. Chen, H. Zhang, and S. Chen, *Flame propagation in a tube with wall quenching of radicals*. Combust. Flame 160 (2013), pp. 2810–2819.
[22] J. Kariuki, J.R. Dawson, and E. Mastorakos, *Measurements in turbulent premixed bluff body flames close to blow-off*. Combust. Flame 159 (2012), pp. 2589–2607.
[23] S. Chaudhuri, S. Kostka, M.W. Renfro, and B.M. Cetegen, *Blowoff dynamics of bluff body stabilized turbulent premixed flames*. Combust. Flame 157 (2010), pp. 790–802.
[24] A. Linan and F.A. Williams, *Fundamental aspect of combustion*. Oxford University Press, New York, 1993.
[25] Y.B. Zeldovich, G.I. Barenblatt, V.B. Librovich, and G.M. Makhviladze, *The mathematical theory of combustion and explosions*. Consultants Bureau, New York, 1985.
[26] J.W. Dold, R.W. Thatcher, A. Omon-Arancibia, and J. Redman, *From one-step to chain-branching premixed flame asymptotics*. Proc. Combust. Inst. 29 (2002), pp. 1519–1926.
[27] J.W. Dold, R.O. Weber, R.W. Thatcher, and A.A. Shah, *Flame balls with thermally sensitive intermediate kinetics*. Combust. Theory Model. 7 (2003), pp. 175–203.
[28] J. Dold, J. Daou, and R. Weber, *Reactive–diffusive stability of premixed flames with modified Zeldovich–Linán kinetics*, in *Simplicity, Rigor and Relevance in Fluid Mechanics*, F.J. Higuera, J. Jimáenez and J.M. Vega, eds., Barcelona, Spain, 2004.

[29] J.W. Dold. *Premixed flames modelled with thermally sensitive intermediate branching kinetics*. Combust. Theory Model. 11 (2007), pp. 909–948.
[30] V.V. Gubernov, H.S. Sidhu, and G.N. Mercer, *Combustion waves in a model with chain branching reaction and their stability*. Combust. Theory Model. 12 (2008), pp. 407–431.
[31] V.V. Gubernov, H.S. Sidhu, G.N. Mercer, A.V. Kolobov, and A.A. Polezhaev, *The effect of Lewis number variation on combustion waves in a model with chain-branching reaction*. J. Math. Chem. 44 (2008), pp. 816–830.
[32] V.V. Gubernov, A.V. Kolobov, A.A. Polezhaev, and H.S. Sidhu, *Stability of combustion waves in the Zeldovich–Liñán model*. Combust. Flame 159 (2012), pp. 1185–1196.
[33] G.J. Sharpe, and S.A.E.G. Falle. *Numerical simulations of premixed flame cellular instability for a simple chain-branching model*. Combust. Flame 158 (2011), pp. 925–934.
[34] H. Li, H. Zhang, and Z. Chen. *Effects of endothermic chain-branching reaction on spherical flame initiation and propagation*, Int. Colloq. Dyn. Explos. React. Syst., Boston, MA, 2017.
[35] H. Zhang, P. Guo, and Z. Chen. *Outwardly propagating spherical flames with thermally sensitive intermediate kinetics and radiative loss*. Combust. Sci. Technol. 185 (2013), pp. 226–248.
[36] Y. Ju, G. Masuya, F. Liu, Y. Hattori, and D. Riechelmann, *Asymptotic analysis of radiation extinction of stretched premixed flames*. Int. J. Heat Mass Transf. 43 (2000), pp. 231–239.
[37] G. Joulin and P. Clavin, *Linear stability analysis of nonadiabatic flames: Diffusional-thermal model*. Combust. Flame 35 (1979), pp. 139–153.
[38] J.K. Hale and H. Kocak, *Dynamics and bifurcations*, 1st ed., New York: Springer-Verlag, New York, 1991.